

# Improvement of a Global High-Resolution Ammonia Emission Inventory for Combustion and Industrial Sources with New Data from the Residential and Transportation Sectors

Wenjun Meng,<sup>†</sup> Qirui Zhong,<sup>†</sup> Xiao Yun,<sup>†</sup> Xi Zhu,<sup>†</sup> Tianbo Huang,<sup>†</sup> Huizhong Shen,<sup>†</sup> Yilin Chen,<sup>†</sup> Han Chen,<sup>†</sup> Feng Zhou,<sup>†</sup> Junfeng Liu,<sup>†</sup> Xinming Wang,<sup>‡</sup> Eddy Y. Zeng,<sup>§</sup> and Shu Tao<sup>\*,†</sup>

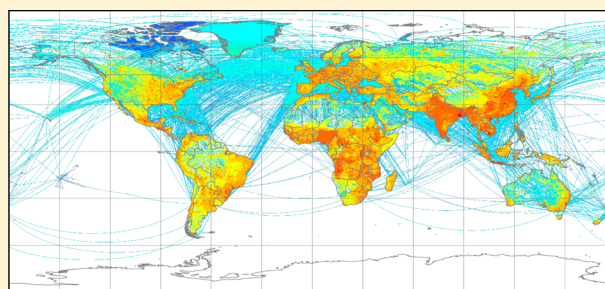
<sup>†</sup>College of Urban and Environmental Sciences, Peking University, Beijing 100871, China

<sup>‡</sup>Guangzhou Institute of Geochemistry, Chinese Academy of Sciences, Guangzhou, 51064, China

<sup>§</sup>School of Environment, Guangzhou Key Laboratory of Environmental Exposure and Health and Guangdong Key Laboratory of Environmental Pollution and Health, Jinan University, Guangzhou 510632, China

## Supporting Information

**ABSTRACT:** There is increasing evidence indicating the critical role of ammonia ( $\text{NH}_3$ ) in the formation of secondary aerosols. Therefore, high quality  $\text{NH}_3$  emission inventory is important for modeling particulate matter in the atmosphere. Unfortunately, without directly measured emission factors (EFs) in developing countries, using data from developed countries could result in an underestimation of these emissions. A series of newly reported EFs for China provide an opportunity to update the  $\text{NH}_3$  emission inventory. In addition, a recently released fuel consumption data product has allowed for a multisource, high-resolution inventory to be assembled. In this study, an improved global  $\text{NH}_3$  emission inventory for combustion and industrial sources with high sectorial (70 sources), spatial ( $0.1^\circ \times 0.1^\circ$ ), and temporal (monthly) resolutions was compiled for the years 1960 to 2013. The estimated emissions from transportation (1.59 Tg) sectors in 2010 was 2.2 times higher than those of previous reports. The spatial variation of the emissions was associated with population, gross domestic production, and temperature. Unlike other major air pollutants,  $\text{NH}_3$  emissions continue to increase, even in developed countries, which is likely caused by an increased use of biomass fuel in the residential sector. The emissions density of  $\text{NH}_3$  in urban areas is an order of magnitude higher than in rural areas.



## INTRODUCTION

Air pollution is a major environmental concern for large transition economies, primarily because of rapid industrialization, high population density, and poor implementation of environmental legislation.<sup>1</sup> It is well-known that air pollution can severely impact health by causing respiratory disease, heart disease, stroke, and cancer.<sup>2</sup> According to the latest estimates, global ambient air pollution alone can cause more than three million premature deaths each year.<sup>3</sup> Although ambient  $\text{NH}_3$  concentrations are much lower than those of major air pollutants, such as sulfur dioxide, ambient  $\text{NH}_3$  not only contributes to inorganic  $\text{PM}_{2.5}$  (particulate matter with an aerodynamic diameter of less than  $2.5 \mu\text{m}$ ) directly but also plays an important role in secondary organic aerosol formation by interacting with gaseous phase organic acids and forming condensable salts.<sup>4</sup>

$\text{NH}_3$  is emitted mainly from livestock, fertilizers, fuel burning, natural vegetation, and the ocean.<sup>5</sup> To quantify its emission, emission inventories have been compiled and used for modeling and assessment. The first of the three global-scale inventories of  $\text{NH}_3$  was developed by Bouwman et al. in 1990. This  $1^\circ \times 1^\circ$  inventory considers the major sources of  $\text{NH}_3$ ,

including data from animal populations, synthetic nitrogen fertilizers, biomass burning, and natural sources.<sup>5</sup> The ACCMIP (Atmospheric Chemistry and Climate Model Intercomparison Project) has developed another global-scale inventory composed of  $0.5^\circ \times 0.5^\circ$  data sets for anthropogenic and biomass burning emissions.<sup>6</sup> The third inventory was developed by the Emissions Database for Global Atmospheric Research (EDGAR) and is the most commonly used. The latest version (v4.3.1) provides estimates of the global  $0.1^\circ \times 0.1^\circ$  anthropogenic emissions from 1970 to 2010 based on publicly available statistics.<sup>7</sup> There are also a number of global-, regional-, and country-scale inventories, such as HTAPv2 ( $0.1^\circ \times 0.1^\circ$ , 2008, 2010) for the globe,<sup>8</sup> NEI ( $0.1^\circ \times 0.1^\circ$ , 2008, 2011 and 2014) for the United States,<sup>9</sup> and REAS ( $1^\circ \times 0.1^\circ$ , 2000–2008),<sup>10</sup> Xin's ( $1 \times 1 \text{ km}$ , 2006)<sup>11</sup> and Cao's ( $0.5^\circ \times 0.5^\circ$ , 2007)<sup>12</sup> inventories for China. Like many other bottom-up emission inventories, a major source of uncertainty of those

Received: July 22, 2016

Revised: January 19, 2017

Accepted: January 25, 2017

Published: January 25, 2017

for  $\text{NH}_3$  inventories is a lack of activity and emission factor (EF) data for developing countries. For example, without directly measured EFs for motor vehicles in developing countries, the EFs previously reported for developed countries were used for developing countries, leading to significant underestimates.<sup>11</sup> Newly published data on both fuel consumption and EFs in developing countries, especially those for the transportation and residential sectors in China,<sup>13–15</sup> provide an opportunity to improve the inventory.

$\text{NH}_3$  emissions from various combustion and industrial sources account for no more than one-fifth of the global total.<sup>5</sup> However, they are critical for air quality modeling and public health assessment because of their contribution to the presence of secondary ammonium in  $\text{PM}_{2.5}$ , particularly in urban areas<sup>16</sup> where most of the exposure and health impacts occur, as well as for their important role in gas-phase clustering<sup>17</sup> and aerosol nucleation and growth,<sup>18–20</sup> especially in the early stage of atmospheric aging of the emissions.  $\text{NH}_3$  mixing ratios down to 100 ppt or less may lead to a more than 100–1000-fold increase in the nucleation rate of sulfuric acid particles.<sup>21</sup> Pre-existing  $\text{NH}_3$  in combustion sources, such as gasoline vehicle exhaust, can greatly enhance new particle formation during photochemical aging immediately after emission.<sup>22</sup>

Recently, global fuel consumption data products (PKU-FUEL) with high sectorial (over 70 sources), spatial ( $0.1^\circ \times 0.1^\circ$ ), and temporal (daily) resolutions have been released,<sup>23,24</sup> and cover the period from 1960 to 2013. These data products were compiled based on subnational energy data (county data for the United States, China, and Mexico; provincial data for eight large countries, including India and Canada; and 0.5 degree data for European countries) from IEA and country databases and disaggregated to 0.1 degree.<sup>23</sup> For the residential sector, a time-for-space substitution method was developed to simulate a monthly variation of electricity use and fuel consumption in individual countries.<sup>24</sup> Based on the product and a newly updated  $\text{NH}_3$  EF database, a high-resolution emission inventory of  $\text{NH}_3$  was compiled for combustion and industrial sources. Source contributions and spatiotemporal variations of the emissions are discussed, and differences between rural and urban areas are addressed.

## MATERIALS AND METHODS

The inventory was compiled through a bottom-up procedure. Fuel consumption and EF data were collected from 70 detailed combustion and industrial sources to include the most recently published literature. The differences in the EFs among countries and years were considered. The uncertainty of the inventory was addressed using a Monte Carlo simulation.

**Emission Sources.** A total of 65 combustions and five industrial sources (i.e., open hearth furnace, catalytic cracking, lime production, fertilizer production, and synthetic ammonia production) were included (Supporting Information (SI) Table S1). The combustion sources were classified into six sectors: power generation, industry, residential sector, transportation, agriculture, and wildfires.

**Fuel Consumption.** Fuel consumption and production data from 1960 to 2011 were obtained from PKU-FUEL, which has subnational energy consumption data for many large countries (e.g., county data for China, the United States, and Mexico; 0.5 degree data for European countries; and provincial/state data for India and Canada) and compiled to reduce the spatial bias caused by the population disaggregation from using country data.<sup>23</sup> The data product covers 70 sources

at a spatial resolution of  $0.1^\circ \times 0.1^\circ$ . In this study, energy data from IEA was added for 2012 and 2013. Since subnational data were not available for these two years, most of our discussions are based on the results for 2011. A set of recently developed models based on the time-for-space substitution method was adopted for simulating monthly variations of energy consumption in the residential sector.<sup>24</sup> In brief, a hypothesis (the same factors affect both spatial and temporal variations of residential energy consumption) was successfully tested, and a set of regression models were developed based on spatial (country or provincial) data and applied to predict temporal (monthly or daily) variations. For wildfire and open-field crop residue burning, the activity data with intra-annual variations were obtained from the Global Fire Emissions Database (GFED).<sup>25,26</sup>

**EFs and Other Data.** EFs for various sources were collected through a thorough literature review (SI Table S1). Large variations among the reported values were expected. A high overall uncertainty includes both spatiotemporal variabilities and true uncertainty (those from measurement and calculation errors). By quantitatively characterizing spatial (among countries) and temporal (interannual and seasonal) variations, the overall uncertainty could be subsequently reduced and the emissions better resolved, both spatially and temporally. Newly published EFs for residential solid fuel combustion and transportation in China were collected and used to replace the previous data that was borrowed from developed countries, resulting in a substantial improvement. It is notable that the remaining uncertainty due to a lack of data for other major developing countries can be further reduced by collecting data from these countries. For emissions from the industrial and energy production sectors, the technology split method was adopted from Bond et al.<sup>27</sup> The ratios of improved woodstoves were obtained from Shen et al.<sup>28</sup> SI Table S1 shows the EFs adopted in this study. Data on population and Gross Domestic Product (GDP) were obtained from the World Bank.<sup>29</sup> Heating degree day (HDD) values were calculated following processes described in Chen.<sup>24</sup>

**Compilation of the Inventory.** Based on fuel consumption and EF data,  $\text{NH}_3$  emissions with  $0.1^\circ \times 0.1^\circ$  and monthly resolutions (residential, wildfire, and open-field crop residue burning) were derived for all sources in 224 countries and territories from 1960 to 2013.

**Data Analysis and Uncertainty Characterization.** SPSS software was used to conduct statistical analysis at a significance level of 0.05. Correlation analysis between residential emissions and population was conducted. A multivariate regression model was used to quantify the dependence of total emissions on temperature and socioeconomic parameters. A Monte Carlo simulation was used to simulate the overall uncertainty. To calculate emissions from a given activity as a product of two multipliers of fuel consumption and EF, the multipliers were randomly generated from a priori uncertainty distributions with given coefficients of variation (CVs); the output distribution was created after 1000 calculations. The CVs of the EFs (241%) and energy consumptions (17.4%), which were obtained from our database, suggested that variations in the EFs were the largest contributors to the overall uncertainty, partially because EFs for residential and transportation sectors in China were used for all developing countries. When the technology split method was used for the activities with a combined EF value derived from EFs of specific technologies, the CV for the technology split ratios, which were obtained

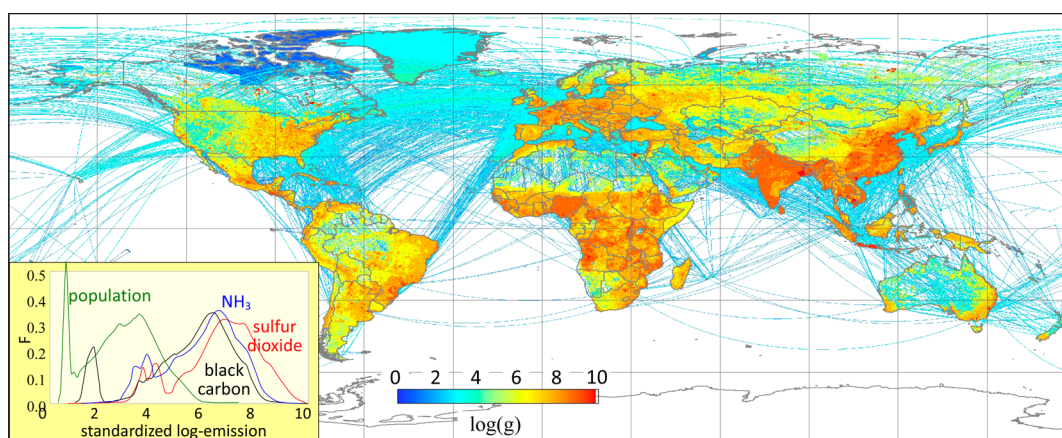


**Figure 1.** Geographical distribution of  $\text{NH}_3$  emissions from combustion and industrial sources. Frequency distributions of  $\text{NH}_3$ , sulfur dioxide, and black carbon emissions of all grids are compared in the inserted panel in the bottom-left corner. The distributions were based on log-transformed and standardized grid data.

from our database, was 1.59%. The medians and interquartile ranges derived from the simulations were used to estimate emissions and characterize the uncertainty of the results, respectively.

## RESULTS AND DISCUSSION

**$\text{NH}_3$  Emissions from Combustion and Industrial Sources.** The global total emission of  $\text{NH}_3$  from combustion and industrial sources was 8.77 Tg (5.05–18.7 Tg, as the interquartile range) in 2011. The relative contribution of these sources to the total of all sources was 11.8% in 2010.<sup>7</sup> Although they accounted for approximately one-eighth of overall  $\text{NH}_3$  emissions, these sources dominate the emissions in urban areas and rural villages, where the majority of people live. In addition, they contributed significantly to the seasonal variations of emissions, a fact that is critical for chemical transport modeling.

In comparison with the inventory from EDGARv4.3.1 (7.53 Tg for 2010, biomass burning was excluded in the latest version of EDGAR4.3.1), our data (5.92 Tg) are 21.4% lower.<sup>7</sup> Large differences were identified in the detailed source profiles. The major differences occur in transportation and residential sectors. Emissions for transportation (1.59 Tg) sectors derived in this study is 2.2 times higher than those in EDGAR (0.50 Tg). This difference likely occurs because the recently reported EFs for China were used to replace the data previously borrowed from developed countries. In addition, residential fuel consumption data in China was fully updated based on a large-scale survey that included over 34 000 households. Based on the activity data from GFED,<sup>26</sup> our estimate of wildfire emission (2008) is 3.17 Tg. In contrast, the value in EDGAR v4.2 is 5.98 Tg, which is 87% higher than our value.<sup>7</sup> In fact, our estimate of  $\text{NH}_3$  emissions from wildfire and deforestation fire (3.44 Tg in 2011) was very close to that provided by GFED (3.39 Tg).<sup>30</sup> Such differences in residential, transportation, and wildfire emissions would explain a substantial difference in spatial distribution. Notably, the total  $\text{NH}_3$  emissions from all anthropogenic combustion sources (5.82 Tg in 2011) is approximately 340% of that reported by the ACCMIP (1.67 Tg).<sup>6</sup> Without having access to the detailed data and calculations that were used in the ACCMIP, we suggest that this difference is due to the varying EFs for developing countries. A result similar to that of ACCMIP<sup>6</sup> would be derived if we simply borrowed the EFs from developed

countries to calculate emissions in developing countries. A detailed comparison can be found in SI Figure S1. It is expected that the calculated emissions for developing countries are more accurate when EFs are directly measured in developing countries instead of using EFs that are borrowed from developed countries.

The relative contributions of major anthropogenic sectors to  $\text{NH}_3$  emissions in 2011 are shown in SI Figure S1, where data for the global total, developing countries and developed countries are presented individually. Detailed source data for 2011 are found in SI Table S2, and multiple year and seasonal data will be available soon at <http://inventory.pku.edu.cn/>. Globally, the residential sector accounted for almost half of the total combustion and industrial emissions, which was dominated by biomass fuel burning. In fact, the residential sector is not only the major emission source of anthropogenic combustion  $\text{NH}_3$  but also the major source of uncertainty in emission estimates because of the high uncertainty in both fuel consumption and EFs. According to our estimates, the uncertainty of  $\text{NH}_3$  EFs for the residential and industrial emission sources is as high as 205% in terms of CV, which is largely caused by the high variation in EF values reported in the literature. In addition, the source profiles were varied between the developed and developing countries, though emissions from the residential sectors ranked first for both. The relative contribution of industrial sources in developed countries is more important than in developing countries. Although transportation is a much more important source in developing countries than in developed countries, the total number of vehicles in the former was less than that in the latter.

**Geographical Variation and Differences among Countries.** With highly spatially resolved fuel consumption data products (PKU-FUEL) and a country-specific EF database available for all sources,  $\text{NH}_3$  global emissions from combustion and industrial sources were mapped for each of the 70 sources at a  $0.1^\circ \times 0.1^\circ$  resolution. Using Monte Carlo simulations, a distribution, instead of a single number, was generated for each of the  $0.1^\circ \times 0.1^\circ$  grids, providing valuable information for further uncertainty analysis. A map of the annual global total  $\text{NH}_3$  emissions from combustion and industrial sources is shown in Figure 1 for 2011 (detailed spatial data are not available for 2012 and 2013). The map can be separated into 70 layers, which, in turn, can be recombined into various source

categories for different purposes. Such flexibility is valuable for making decisions when mitigation measures must be taken for specific sources. Similar to other major air pollutants, such as sulfur dioxide and black carbon,<sup>15</sup> hot areas of anthropogenic NH<sub>3</sub> emissions from combustion and industrial sources can be identified for regions with high population densities, including eastern China, the Indian subcontinent, Brazil, central Africa, West Europe, and the eastern United States. Nevertheless, as shown in the frequency distribution diagram in Figure 1 (inserted panel in the left-bottom corner), a central tendency of combustion and industrial NH<sub>3</sub> emissions was similar to that of black carbon but not as strong as that of sulfur dioxide, which is likely due to a heavy contribution from residential sources.

Although the total emissions were generally dependent on the population density, significant spatial variation in per-capita emissions can still be observed, as shown in SI Figure S2 for 2011. The spatial variation of per-capita emissions was much less than that of the emission density. In fact, the calculated CVs were 123% and 30% for emission densities and per-capita emissions, respectively, indicating the total population as a dominant influence. The spatial difference in per-capita emissions was likely caused by temperature and the source profile pattern. In general, per-capita emissions in cold regions were much higher than those in warm regions because more fuel is required for heating the cold areas in the winter. Typical examples were relatively high per-capita emissions in north China, north Europe, and the southern region of South America in comparison to other areas of China, south Europe, and northern regions of South America, respectively. A typical example of source profile influence can be observed in Southeast Asia, where heating activities are not required at all, but biomass emissions are dominated by cooking fuels.<sup>31</sup> This was also true for France.<sup>32</sup>

The influence of these two factors can be quantified by conducting a multivariate regression analysis and testing the significance of the independent variables. The temperature associated with heating can be expressed by HDD values (degree-day). The energy mix and, consequently, the emission profile were strongly associated with economic development, which can be quantified by per-capita GDP (GDP<sub>cap</sub>, USD) and urbanization rate (U, %, increasing rate of urban population). The total anthropogenic NH<sub>3</sub> emissions from combustion and industrial sources ( $E_{\text{total}}$ , logGg) can be quantified using the following equation for individual countries based on the standardized data:

$$E_{\text{total}} = 0.025\log(\text{GDP}_{\text{cap}}) + 0.978P + 0.003U + 0.007\text{HDD} + 0.003$$

$$R^2 = 0.976$$

Where,  $P$  (people) is population, and over 97% of the variation among countries can be explained by these parameters. The predominant influence of total population is expected, as it is consistent with the significant difference between the calculated CVs for total and per-capita emissions. If residential and nonresidential sectors are modeled separately, emissions from the nonresidential sector are mainly affected by economic development in addition to population. Both the urbanization rate and HDD values have positive influences on residential emissions because of differences in the energy mix between urban and rural residents, as well as heating needs. The small but positive slope of  $U$  is likely due to an increase in

transportation fuel consumption. It should be noted that the possibility of multicollinearity in the model cannot be completely excluded.

$$E_{\text{residential}} = -0.009\log(\text{GDP}_{\text{cap}}) + 0.968P + 0.037U + 0.019\text{HDD} - 0.006$$

$$R^2 = 0.971$$

$$E_{\text{non-residential}} = 0.064\log(\text{GDP}_{\text{cap}}) + 0.917P - 8.88 \times 10^8$$

$$R^2 = 0.841$$

Similar relationships have been reported for energy consumption and emissions of other pollutants.<sup>24</sup> In 2011, developing countries contributed more than five times (5.17 Tg) the total anthropogenic emissions from combustion and industrial sources in developed countries (0.88 Tg). The anthropogenic emissions in developing countries were dominated by solid fuels, especially biomass burning in the residential sector (46.6% of the total anthropogenic sources), followed by the transportation sector (29.7%); both were significantly underestimated in previous studies, likely because of a lack of EF data for developing countries. The difference in per-capita anthropogenic NH<sub>3</sub> emissions between developing (0.92 kg/cap) and developed countries (0.85 kg/cap) was smaller than that of the total emissions (1.36 vs 1.27 kg/cap) because of the larger population in developing countries.

SI Figure S3 shows the geographical distributions of emission intensities in terms of energy consumption (g/GJ) (top panel) and GDP (g/USD) (bottom panel). Globally, the average emission intensities in terms of energy consumption and GDP were 19.0 g/GJ and 0.027 g/USD in 2011, respectively. The differences in emission intensities among countries, particularly between developed (8.74 g/GJ and 0.014 g/USD) and developing (34.53 g/GJ and 0.041 g/USD) countries, were dramatic, indicating large differences in population, energy mix, and energy efficiency.<sup>33</sup> For example, the large differences in overall emission intensities between China (11.9 g/GJ and 0.12 g/USD) and India (23.5 g/GJ and 0.20 g/USD) were largely caused by their differences in residential emission intensities (i.e., 52.4 g/GJ and 0.027 g/USD for China, and 64.5 g/GJ and 0.054 g/USD for India).

Source profiles of total NH<sub>3</sub> emissions for 12 world regions are shown in Figure 2. All 70 sources are combined into six sectors, and detailed information on all sources is listed in SI

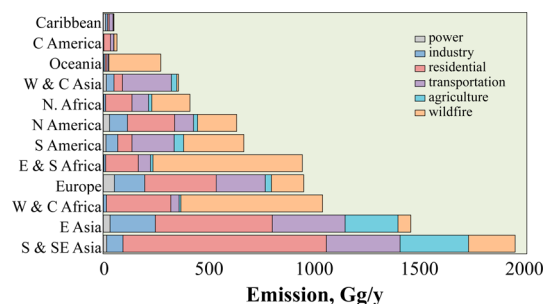


**Figure 2.** Source profiles of total NH<sub>3</sub> emissions for 12 regions including the Caribbean, Central America, Oceania, West and Central Africa, North Africa, North America, South America, East and South Africa, Europe, West and Central Africa, East Asia, and South and Southeast Asia.

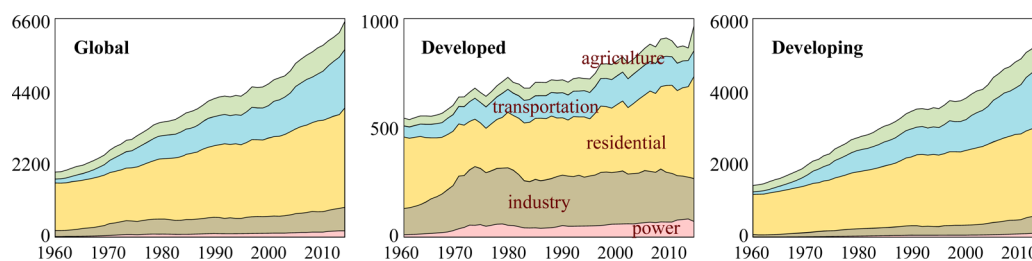


**Figure 3.** Historical changes in  $\text{NH}_3$  emissions from combustion and industrial sources for the world (left panel), developed countries (middle panel), and developing countries (right panel) from 1960 to 2013. Emissions from the five main sectors, including agriculture, transportation, residential, industry, and energy, are shown as stacked area charts.

**Table S3.** Wildfire accounted for a large portion of the emissions in Oceania, Africa, and South America.<sup>26</sup> Residential sources were the largest contributors to emissions in Asia and Europe due to high population densities. The highest contribution from transportation occurred in West and Central Asia, and residential emissions also ranked first in Europe, where approximately a quarter of the total energy consumption occurred in this sector.<sup>31,32</sup> The contribution from industry was relatively high in East Asia, including China. Such detailed source information can provide valuable information for those involved in formulating abatement strategies.

**Temporal Trends of Anthropogenic Combustion and Industrial Emissions.** Historically, emissions of  $\text{NH}_3$  from anthropogenic combustion and industrial sources increased steadily from 1960 to 2013. Figure 3 shows the temporal trends of the annual total and sectorial emissions from anthropogenic sources for all countries (left panel), developed countries (middle panel), and developing countries (right panel). For most other air pollutants, including sulfur dioxide, primary particulate matter, black carbon, and polycyclic aromatic hydrocarbons, emissions reached their peak in the 1970s and have since declined.<sup>15,28,33,34</sup> Such global trends were mainly driven by efforts to reduce emissions in developed countries since the Clean Air Act was enacted in the United States in the 1970s.<sup>35</sup> However,  $\text{NH}_3$  appears to be an exception. Although its emission from power stations and industrial sources stopped increasing after the early 1970s and even decreased after the 2008 recession, total  $\text{NH}_3$  emissions have continued to increase greatly because of increased emissions from the residential sector. In the residential sector, this trend can be explained by the increased use of biomass fuel in European countries, such as Germany. For transportation, the rapid emissions increase in developing countries was driven by an expansion of the vehicle fleet. In developed countries, the transportation emissions of  $\text{NH}_3$  did not change much over these years, while the emissions of other pollutants from transportation generally decreased. This can be explained by the introduction of a selective catalytic reduction technology for motor vehicles, which can reduce  $\text{NO}_x$  but leads to increased  $\text{NH}_3$  emissions.<sup>36</sup> Although the total emissions declined slightly after 2008, primarily caused by the steady decrease in industrial emissions, the trend reversed and emissions increased again, driven by increasing emissions from the residential sector. In terms of  $\text{NH}_3$  emission, it appears that even developed countries have not reached the peak of the environmental Kuznets curve.<sup>37</sup> At the same time, developing countries were experiencing the early stages of the environmental Kuznets curve with an increasing pace.

Population growth is the major cause of the emissions increase in the residential sector. In fact, significant correlations were found between residential emissions and total population

for both developing ( $p < 0.001$ ) and developed ( $p < 0.001$ ) countries. This is consistent with the influence of population on spatial variation, as discussed in the last section. Even more quickly increasing trends in the industrial and transportation sectors are caused by the expansion of industrial facilities and the number of motor vehicles as a consequence of rapid economic development. For example, the total number of private cars in China increased from 224 thousand in 1960 to 105 million in 2013,<sup>38</sup> and industrial output increased from 0.165 to 56.9 trillion RMB during the same period.<sup>39</sup> These driving forces are almost identical to those that led the spatial variation quantified in the last section. Chen et al. successfully tested a hypothesis in which both spatial and temporal variations of energy consumption and pollutant emissions were affected by the same sets of factors.<sup>24</sup> This hypothesis was further confirmed by the similarity in the factors that affect both the spatial and temporal differences in  $\text{NH}_3$  emissions observed in this study. It appears that this global trend will continue in the future if residential emission intensity in major countries is not substantially decreased, which is much more difficult than controlling nonresidential sources.

As typical examples, changes in the sectorial emissions of  $\text{NH}_3$  in the United States, China, India, Argentina, and Germany are shown in SI Figure S4. Compared with the overall trend for developed countries, the total emissions in the United States began to decrease after 2007, whereas the emissions in most other developed countries continued to increase until 2013, driven by an increase in emissions from the residential sector. Unlike those in the United States, residential emissions in Europe (e.g., Germany) were relatively high and continued to increase, which was likely caused by the expansion of biomass fuel use since the 1980s as a part of the effort to reduce carbon emissions by using more carbon neutral fuels.<sup>31</sup> As expected, the trends observed for the developing countries are similar to those in China and India. However, emissions in both the residential and agricultural sectors in China have leveled off since the early 1990s in large part due to rapid industrialization and urbanization, which further led to a recent accelerated increase in industrial emissions. At the same time, emissions from the transportation sector grew quickly because of a rapid increase in the total number of vehicles on the road. Additionally, emissions from various sectors in India continued to increase steadily. Notably, the trend for India was very similar to that in China before the 1990s. The emissions were also energy mix dependent. For example, the residential sector in Argentina (IEA) is rich in oil and natural gas reserves, thus almost no coal or biomass fuels were used,<sup>31</sup> leading to very low residential emissions. Global emissions of  $\text{NH}_3$  from non-combustion and nonindustrial sources, including livestock and farming, followed a generally similar trend as those from

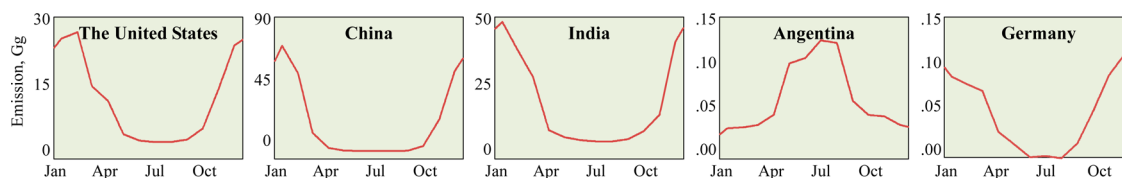


**Figure 4.** Seasonal variations of  $\text{NH}_3$  emissions in 2011 from residential fuel combustions in several representative countries.

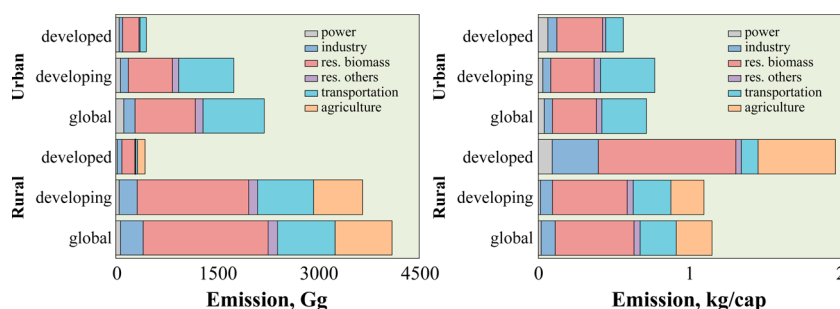


**Figure 5.** Comparison of emissions from various sectors between urban and rural areas. The comparisons are performed for all countries (global), developing countries, and developed countries.

combustion sources over the same time period.<sup>7</sup> Therefore, the relative contributions of combustion and industrial sources to the overall anthropogenic emissions were more or less constant, varying from 11.6% to 13.2% with a mean and standard deviation of 12.2% and 0.004, respectively (SI Figure S5). In fact, residential fuel consumption, livestock, and agricultural production are driven by similar anthropogenic factors of population and economic growth<sup>24</sup> and are relatively difficult to abate in comparison with industrial and power generation sources.

For modeling purposes, data on daily, or even hourly, emissions are required. This is particularly important for  $\text{NH}_3$ , which plays a critical role in the formation of secondary aerosols during severe pollution episodes.<sup>4</sup> Among the various emission sources, residential sectors, open-field crop residue burning, and wildfires are the major contributors to seasonality among all combustion sources. Of these, fuel consumption from open-field crop residue burning and wildfires can be obtained from remote sensing data.<sup>40,41</sup> Consequently, there exists a major data gap in the residential sector because it is a major source of  $\text{NH}_3$  combustion emissions. Unfortunately, residential energy consumption data are only available on an annual basis (IEA),<sup>31</sup> and monthly and daily data are seldom recorded. Recently, a set of regression models were developed for simulating intra-annual trends of residential energy consumption on the global scale by using a space-for-time substitution method.<sup>24</sup> These models were adopted in this study to calculate monthly residential emissions of  $\text{NH}_3$  for all individual countries. Several examples of monthly residential emissions are presented in Figure 4 for China, the United States, India, Argentina, and Germany in 2011, all of which show strong seasonality. Because emissions from power generation are relatively small, only residential fuels were considered. For all countries shown here, a single peak can be found in winter when heating is required. With the models available, daily variations can also be modeled when the input data, including HDD values, are available.

As mentioned previously, residential fuel consumption, open-field crop residue burning, and wildfires are major sources of seasonal changes in emissions. The seasonal and multiyear trends of emissions from these activities are compared in SI

Figure S6, using the data from 2011. It appears that wildfire emissions had a much larger variation than those of both the residential sectors and open-field crop residue burning in terms of both intra-annual (left panel) and interannual (right panel) variations.

In addition to time trends in global total emissions, the geographical variations of annual emissions changed over time. Such changes are illustrated in SI Figure S7 as the geographical distributions of normalized global emissions from all combustion and industrial sources, except wildfire, in 2002 and 2011 as two sample years. The frequency distributions of the normalized emissions are also shown in the inserted panel in SI Figure S7. There are notable changes in the spatial distributions between the two years, and significant differences in Africa, South America, China, India, and Southeast Asia can be clearly observed. The largest peaks of the frequency distributions, which represent emissions in China and India, were reduced slightly over the decade. The reduction of emissions also occurred in developed countries. For example, a very low peak of emissions in 2011, corresponding to the western United States and Brazil, was shifted left.

**Emissions in Urban and Rural Areas.** The high spatial resolution of the emission inventory enables us to distinguish emissions between urban and rural areas.<sup>23</sup> Figure 5 shows rural and urban total (left panel) and per-capita (right panel)  $\text{NH}_3$  emissions from anthropogenic combustion and industrial sources in developing countries, developed countries and the entire world. The contributions of the major source sectors to emissions are shown as stacked bars. Globally, the emissions in urban and rural areas in 2011 were 2.20 and 4.09 Tg, respectively. The main difference was caused by emissions from the residential and agricultural sectors, and the latter occurred only in the rural areas. The patterns are very different for per-capita emissions, and the difference between rural (1.14 kg/cap) and urban (0.71 kg/cap) areas was relatively small. There was a large difference between rural and urban areas in developed countries, which is primarily caused by high per-capita emissions from the agricultural and residential sectors, and industrial processes. Regarding transportation, per-capita emissions from urban areas were higher than those from rural areas in both developing and developed countries.

Typical examples of the differences in anthropogenic combustion and industrial emissions between rural and urban areas are shown in SI Figure S8 for China, the United States, India, Argentina, and Germany in 2011. The difference among countries is obvious. In China, residential sectors contributed significantly to emissions for both the urban (53.5%) and rural (33.1%) areas. The relatively high contribution in rural areas was caused by large emissions from agricultural activity (26.8%), transportation (23.7%), and residential biomass burning (33.1%). In India, residential emissions contributed even larger fractions to both the urban (67.3%) and rural (63.0%) areas. For the United States, residential emissions ranked first in urban areas (47.1%), followed by transportation emissions (42.7%). In urban areas of Argentina, power plant emissions ranked first (31.7%), followed by residential emissions (29.9%), and then transportation (25.2%). Nevertheless, agricultural emissions in Argentina's rural areas dominated the profile (97.8%). Residential biomass burning was also the dominant sector for both urban (54.5%) and rural areas (47.1%) in Germany.

Because urban areas occupy a much smaller fraction of total land area, emission densities of  $\text{NH}_3$  in urban areas of both developed (274.71  $\text{Tg}/\text{km}^2$ ) and developing (623.48  $\text{Tg}/\text{km}^2$ ) countries are more than 1 order of magnitude higher than those in rural areas (11.58  $\text{Tg}/\text{km}^2$  and 39.29  $\text{Tg}/\text{km}^2$  for developed and developing countries, respectively).

As the most abundant alkaline trace gas in the atmosphere,  $\text{NH}_3$  plays a vital role in forming fine particles of light-scattering sulfates and nitrates through acid–base neutralization.<sup>19,46</sup> It also regulates particle acidity, which is vital in both the aqueous phase oxidation of  $\text{SO}_2$ <sup>45</sup> and the heterogeneous formation of secondary organic aerosols.<sup>47,48</sup> As discussed previously, the combustion/industrial  $\text{NH}_3$  emissions are largely driven by population, typically peak in wintertime and have much higher densities in urban areas than in rural areas. These characteristic emission patterns make combustion/industrial  $\text{NH}_3$  emissions important in atmospheric chemistry, particularly in densely populated and highly industrialized urban areas and in the winter, when episodes of heavy haze occur frequently in megacities such as China's capital, Beijing. In China's Beijing-Tianjin-Hebei region, residential emission of primary  $\text{PM}_{2.5}$  and carbonaceous aerosols might dominate over other emission sources during a heavily polluted winter.<sup>49</sup> However, the role of residential  $\text{NH}_3$  emission, which is the largest contributor of combustion/industrial  $\text{NH}_3$  emissions, is still not fully understood. In the frozen winters of North China,  $\text{NH}_3$  emissions from livestock and fertilizer decrease and residential emissions reach an annual maximum, thus becoming comparatively distinctive. A recent study confirmed that fossil fuel combustion-related emissions dominated atmospheric ammonia sources in urban Beijing during severe haze episodes in the winter of 2013, as evidenced by stable nitrogen isotopes.<sup>50</sup> Additionally, in east China's megacity, Shanghai, higher  $\text{NH}_3$  concentrations were observed during the summer because of intense emissions from temperature-dependent agricultural sources, while  $\text{NH}_3$  pollution events in spring were associated with the burning of crop residues, and elevated  $\text{NH}_3$  concentrations in winter were largely due to climate-independent vehicle emission.<sup>16</sup> The updated combustion/industrial  $\text{NH}_3$  emission inventory in this study can be of great help for developing an observation- or model-based in-depth understanding of air pollution in megacities, regional air quality and climate effects induced by air pollutants.<sup>42–44</sup>

## ■ ASSOCIATED CONTENT

### § Supporting Information

The Supporting Information is available free of charge on the ACS Publications website at DOI: 10.1021/acs.est.6b03694.

Detailed source profiles for various regions, geographical distribution of per-capita emissions and emission intensities, temporal trends of emissions in major countries and relative contributions of combustion emissions, and differences in emissions between rural and urban areas (PDF)

## ■ AUTHOR INFORMATION

### Corresponding Author

\*Phone/fax: +86-10-62751938; e-mail: taos@pku.edu.cn.

### ORCID

Feng Zhou: 0000-0001-6122-0611

Shu Tao: 0000-0002-7374-7063

### Notes

The authors declare no competing financial interest.

## ■ ACKNOWLEDGMENTS

This work was supported by the National Natural Science Foundation of China (41390240 and 41571130010).

## ■ REFERENCES

- (1) Feng, L.; Liao, W. J. Legislation, plans, and policies for prevention and control of air pollution in China: achievements, challenges, and improvements. *J. Cleaner Prod.* **2016**, *112* (2), 1549–1558.
- (2) Fang, M.; Chan, C. K.; Yao, X. Managing air quality in a rapidly developing nation: China. *Atmos. Environ.* **2009**, *43* (1), 79–86.
- (3) Global Burden of Disease Study 2013 (GBD 2013). *Results by Location, Cause, and Risk Factor*; Institute for Health Metrics and Evaluation (IHME): Seattle, United States, 2016.
- (4) Na, K.; Song, C.; Switzer, C.; Cocker, D. R. Effect of ammonia on secondary organic aerosol formation from  $\alpha$ -pinene ozonolysis in dry and humid conditions. *Environ. Sci. Technol.* **2007**, *41* (17), 6096–6102.
- (5) Bouwman, A. F.; Lee, D. S.; Asman, W. A. H.; Dentener, F. J.; Van Der Hoek, K. W.; Olivier, J. G. J. A global high-resolution emission inventory for ammonia. *Global Biogeochem. Cycles* **1997**, *11* (4), 561–587.
- (6) ACCMIP data [Online]; [http://accmip-emis.iek.fz-juelich.de/data/accmip/gridded\\_netcdf/accmip\\_maccity\\_biomassburning/](http://accmip-emis.iek.fz-juelich.de/data/accmip/gridded_netcdf/accmip_maccity_biomassburning/). (accessed July 10, 2016).
- (7) Emissions Database for Global Atmospheric Research (EDGAR v4.3.1) [Online]; <http://edgar.jrc.ec.europa.eu/overview.php?v=431>. (accessed January 6, 2017).
- (8) Hemispheric Transport of Air Pollution (HTAP v2) [Online]; <http://www.htap.org/>. (accessed July 16, 2016).
- (9) 2011 National Emission Inventory (NEI) Documentation [Online]; <https://www.epa.gov/air-emissions-inventories/2011-national-emissions-inventory-nei-documentation>. (accessed January 5, 2017).
- (10) Klimont, Z. Current and future emissions of ammonia in China, in *10th Annual Emission Inventory Conference: One Atmosphere, One Inventory, Many Challenges*; Denver: The United States, May, 2001; pp 1–3.
- (11) Huang, X.; Song, Y.; Li, M. M.; Li, J. F.; Huo, Q.; Cai, X. H.; Zhu, T.; Hu, M.; Zhang, H. S. A high-resolution ammonia emission inventory in China. *Global Biogeochem. Cycles* **2012**, *26* (1), 239256.
- (12) Cao, G. L.; Zhang, X. Y.; Gong, S. L.; An, X. Q.; Wang, Y. Q. Emission inventories of primary particles and pollutant gases for China. *Chin. Sci. Bull.* **2011**, *56* (8), 781–788.
- (13) Liu, T. Y.; Wang, X. M.; Wang, B. G.; Ding, X.; Deng, W.; Lv, S. J.; Zhang, Y. L. Emission factor of ammonia ( $\text{NH}_3$ ) from on-road

vehicles in China: tunnel tests in urban Guangzhou. *Environ. Res. Lett.* **2014**, *9* (6); DOI: 06402710.1088/1748-9326/9/6/064027.

(14) Sun, K.; Tao, L.; Miller, D. J.; Khan, M. A.; Zondlo, M. A. On-road ammonia emissions characterized by mobile, open-path measurements. *Environ. Sci. Technol.* **2014**, *48* (7), 3943–50.

(15) Wang, R.; Tao, S.; Shen, H. Z.; Huang, Y.; Chen, H.; Balkanski, Y.; Boucher, O.; Ciais, P.; Shen, G. F.; Li, W.; Zhang, Y. Y.; Chen, Y. C.; Lin, N.; Su, S.; Li, B. G.; Liu, J. F.; Liu, W. X. Trend in global black carbon emissions from 1960 to 2007. *Environ. Sci. Technol.* **2014**, *48* (12), 6780–6787.

(16) Chang, Y. H.; Zou, Z.; Deng, C. R.; Huang, K.; Collett, J. L.; Lin, J.; Zhuang, G. S. The importance of vehicle emissions as a source of atmospheric ammonia in the megacity of Shanghai. *Atmos. Chem. Phys.* **2016**, *16* (5), 3577–3594.

(17) Schobesberger, S.; Franchin, A.; Bianchi, F.; Rondo, L.; Duplissy, J.; Kürten, A.; Ortega, I. K.; Metzger, A.; Schnitzhofer, R.; Almeida, J. On the composition of ammonia–sulfuric-acid ion clusters during aerosol particle formation. *Atmos. Chem. Phys.* **2015**, *15* (1), 55–78.

(18) Korhonen, P.; Kulmala, M.; Laaksonen, A.; Viisanen, Y.; McGraw, R.; Seinfeld, J. Ternary nucleation of H<sub>2</sub>SO<sub>4</sub>, NH<sub>3</sub>, and H<sub>2</sub>O in the atmosphere. *J. Geophys. Res., [Atmos.]* **1999**, *104* (D21), 26349–26353.

(19) Ortega, I.; Kurtén, T.; Vehkamäki, H.; Kulmala, M. The role of ammonia in sulfuric acid ion induced nucleation. *Atmos. Chem. Phys.* **2008**, *9* (19), 2859–2867.

(20) Benson, D.; Yu, J.; Markovich, A.; Lee, S.-H. Ternary homogeneous nucleation of H<sub>2</sub>SO<sub>4</sub>, NH<sub>3</sub>, and H<sub>2</sub>O under conditions relevant to the lower troposphere. *Atmos. Chem. Phys.* **2011**, *11* (10), 4755–4766.

(21) Kirkby, J.; Curtius, J.; Almeida, J.; Dunne, E.; Duplissy, J.; Ehrhart, S.; Franchin, A.; Gagné, S.; Ickes, L.; Kürten, A. Role of sulphuric acid, ammonia and galactic cosmic rays in atmospheric aerosol nucleation. *Nature (London, U.K.)* **2011**, *476* (7361), 429–433.

(22) Liu, T.; Wang, X.; Deng, W.; Zhang, Y.; Chu, B.; Ding, X.; Hu, Q.; He, H.; Hao, J. Role of ammonia in forming secondary aerosols from gasoline vehicle exhaust. *Sci. China: Chem.* **2015**, *58* (9), 1377–1384.

(23) Wang, R.; Tao, S.; Ciais, P.; Shen, H. Z.; Huang, Y.; Chen, H.; Shen, G. F.; Wang, B.; Li, W.; Zhang, Y. Y.; Lu, Y.; Zhu, D.; Chen, Y. C.; Liu, X. P.; Wang, X. L.; Liu, W. X.; Li, B. G.; Piao, S. L. High-resolution mapping of combustion processes and implications for CO<sub>2</sub> emissions. *Atmos. Chem. Phys. Discuss.* **2012**, *13* (10), 21211–21239.

(24) Chen, H.; Huang, Y.; Shen, H. Z.; Chen, Y. L.; Ru, M. Y.; Chen, Y. C.; Lin, N.; Su, S.; Zhuo, S. J.; Zhong, Q. R.; Wang, X. L.; Liu, J. F.; Li, B. G.; Tao, S. Modeling temporal variations in global residential energy consumption and pollutant emissions. *Appl. Energy* **2015**, *20* (12), 327–340.

(25) van der Werf, G. R.; Randerson, J. T.; Giglio, L.; Collatz, G. J.; Kasibhatla, P.; Sand, A. A. F. Interannual variability in global biomass burning emissions from 1997 to 2004. *Atmos. Chem. Phys.* **2006**, *6* (8), 3423–41.

(26) van der Werf, G. R.; Randerson, J. T.; Giglio, L.; Collatz, G. J.; Mu, M.; Kasibhatla, P. S.; Morton, D. C.; DeFries, R. S.; Jin, Y.; van Leeuwen, T. T. Global fire emissions and the contribution of deforestation, savanna, forest, agriculture, and peat fires. *Atmos. Chem. Phys. Discuss.* **2010**, *10* (23), 16153–16230.

(27) Bond, T. C.; Streets, D. G.; Yarber, K. F.; Nelson, S. M.; Woo, J.; Klimont, Z. A technology-based global inventory of black and organic carbon emissions from combustion. *J. Geophys. Res.* **2004**, *109* (D14), 1149–1165.

(28) Shen, H. Z.; Huang, Y.; Wang, R.; Zhu, D.; Li, W.; Shen, G. F.; Wang, B.; Zhang, Y. Y.; Chen, Y. C.; Lu, Y.; Chen, H.; Li, T. C.; Sun, K.; Li, B. G.; Liu, W. X.; Liu, J. F.; Tao, S. Global atmospheric emissions of polycyclic aromatic hydrocarbons from 1960 to 2008 and future predictions. *Environ. Sci. Technol.* **2013**, *47* (12), 6415–6424.

(29) GDP (current US\$) [Online]; The World Bank; <http://data.worldbank.org/indicator/NY.GDP.MKTP.CD>. (accessed July 10, 2016).

(30) *Global Fire Emissions Database*; [Online]; GFED; <http://www.globalfiredata.org/>. (accessed July 10, 2016).

(31) IEA *World Energy Statistics and Balances* [Online]; OECD iLibrary; International Energy Agency. <http://www.oecd-ilibrary.org/statistics>. (accessed July 10, 2016).

(32) Risch, A.; Salmon, C. What matters in residential energy consumption? Evidence from France. *Econ. Et. Finances* **2013**, *40*, 79.

(33) Huang, Y.; Shen, H. Z.; Chen, H.; Wang, R.; Zhang, Y. Y.; Su, S.; Chen, Y. C.; Lin, N.; Zhuo, S. J.; Zhong, Q. R.; Wang, X. L.; Liu, J. F.; Li, B. G.; Liu, W. X.; Tao, S. Quantification of global primary emissions of PM<sub>2.5</sub>, PM<sub>10</sub>, and TSP from combustion and industrial process sources. *Environ. Sci. Technol.* **2014**, *48* (23), 13834–13843.

(34) Smith, S. J.; Aardenne, J. V.; Klimont, Z.; Andres, R. J.; Volke, A.; Delgado Arias, S. Anthropogenic sulfur dioxide emissions: 1850–2005. *Atmos. Chem. Phys.* **2011**, *11* (3), 1101–1116.

(35) *Lead*; [Online]; U.S. Environmental Protection Agency, Washington DC, <https://www.epa.gov/lead>. (accessed July 16, 2016).

(36) Heeb, N. V.; Forss, A. M.; Brühlmann, S.; Luscher, R.; Saxer, C. J.; Hug, P. Three-way catalyst-induced formation of ammonia velocity and acceleration dependent emission factors. *Atmos. Environ.* **2006**, *40* (31), 5986–5997.

(37) Ciegis, R. The use of the environmental Kuznets curve: environmental and economic implications. *Int. J. Environ. Pollut.* **2008**, *33* (2–3), 313–335.

(38) The National Bureau of statistics of the People's Republic of China; *China Statistical Yearbook*; China Statistics Press: Beijing, China, 2014.

(39) China Industry Yearbook Editorial Committee. *Chinese Industry Yearbook*; Beijing Tech University Press: Beijing, 2014.

(40) Kanabkaew, T.; Oanh, N. T. K. Development of spatial and temporal emission inventory for crop residue field burning. *Environ. Modeling Assess.* **2011**, *16* (5), 453–464.

(41) Stockwell, C. E.; Yokelson, R. J.; Kreidenweis, S. M.; Robinson, A. L.; DeMott, P. J.; Sulliban, R. C.; Reardon, J.; Ryan, K. C.; Griffith, D. W. T.; Stevens, L. Trace gas emissions from combustion of peat, crop residue, biofuels, grasses, and other fuels: configuration and FTIR component of the fourth Fire Lab at Missoula Experiment (FLAME-4). *Atmos. Chem. Phys. Discuss.* **2014**, *14* (18), 10061–10134.

(42) Pan, Y.; Tian, S.; Liu, D.; Fang, Y.; Zhu, X.; Zhang, Q.; Zheng, B.; Michalski, G.; Wang, Y. Fossil fuel combustion-related emissions dominate atmospheric ammonia sources during severe haze episodes: Evidence from 15N-stable isotope in size-resolved aerosol ammonium. *Environ. Sci. Technol.* **2016**, *50* (15), 8049–8056.

(43) Ortega, I. K.; Kurtén, T.; Ki, H. V.; Kulmala, M. The role of ammonia in sulfuric acid ion induced nucleation. *Atmos. Chem. Phys.* **2008**, *8* (11), 2859–2867.

(44) Ye, X.; Ma, Z.; Zhang, J.; Du, H.; Chen, J.; Chen, H.; Yang, X.; Gao, W.; Geng, F. Important role of ammonia on haze formation in Shanghai. *Environ. Res. Lett.* **2011**, *6* (2), 38–746.

(45) Wang, X.; Wang, W.; Yang, L.; Gao, X.; Nie, W.; Yu, Y.; Xu, P.; Zhou, Y.; Wang, Z. The secondary formation of inorganic aerosols in the droplet mode through heterogeneous aqueous reactions under haze conditions. *Atmos. Environ.* **2012**, *63* (1), 68–76.

(46) Ye, X.; Ma, Z.; Zhang, J.; Du, H.; Chen, J.; Chen, H.; Yang, X.; Gao, W.; Geng, F. Important role of ammonia on haze formation in Shanghai. *Environ. Res. Lett.* **2011**, *17* (2), 38–746.

(47) Jang, M.; Czoschke, N. M.; Lee, S.; Kamens, R. M. Heterogeneous atmospheric aerosol production by acid-catalyzed particle-phase reactions. *Science (Washington, DC, U. S.)* **2002**, *298* (5594), 814–817.

(48) Deng, W.; Liu, T. Y.; Zhang, Y. L.; Situ, S. P.; Hu, Q. H.; He, Q. F.; Zhang, Z.; LV, S. J.; Bi, X. H.; Wang, X. M.; Boreave, A.; George, C.; Ding, X.; Wang, X. M. Secondary organic aerosol formation from photo-oxidation of toluene with NO<sub>x</sub> and SO<sub>2</sub>: Chamber simulation with purified air versus urban ambient air as matrix. *Atmos. Environ.* **2017**, *150* (1), 67–76.

(49) Liu, J.; Mauzerall, D. L.; Chen, Q.; Zhang, Q.; Song, Y.; Peng, W.; Klimont, Z.; Qiu, X. H.; Zhang, S. Q.; Hu, M.; Lin, W. L.; Smith, K. R.; Zhu, T. Air pollutant emissions from Chinese households: A major and underappreciated ambient pollution source. *Proc. Natl. Acad. Sci. U. S. A.* **2016**, *113* (28), 7756–7761.

(50) Pan, Y.; Tian, S.; Liu, D.; Fang, Y.; Zhu, X.; Zhang, Q.; Zheng, B.; Michalski, G.; Wang, Y. Fossil fuel combustion-related emissions dominate atmospheric ammonia sources during severe haze episodes: Evidence from  $^{15}\text{N}$ -stable isotope in size-resolved aerosol ammonium. *Environ. Sci. Technol.* **2016**, *50* (15), 8049–8056.